Hydrodynamics of a Lamella Electrosettler

Using the principles of conservation of mass and momentum for each phase, a theory is developed for describing quantitatively the sedimentation of colloidal particles in vessels having electrodes that are inclined to the vertical.

As a limiting case, a kinematic settling formula was derived that describes the motion of settling fronts of colloidal alumina particles suspended in tetralin as a function of angle of inclination and strength of applied electric field in terms of electrophoretic mobilities. A hydrodynamic computer model shows the flow patterns and settling behavior of such lamella settlers with and without an applied electric field. The predicted motions of the settling fronts and the thicknesses of the clear boundary layers above the upper wall of the inclined vessels globally agreed with the experimental observations.

Dimitri Gidaspow
Yang-Tsai Shih
Jacques Bouillard
Darsh Wasan
Department of Chemical Engineering
Illinois Institute of Technology
Chicago, IL 60616

Introduction

Lamella settlers are commonly used industrially for clarification of aqueous and nonaqueous slurries (Forsell and Hedstrom, 1975). Acrivos and Herbolzheimer (1979) present a theory of their operation from a hydrodynamic point of view. They extended the work of Hill et al. (1977) by considering the limit, in which the ratio of the sedimentation Grashof number to the sedimentation Reynolds number becomes asymptotically large. Herbolzheimer and Acrivos (1981) present analytical derivations of laminar profiles in inclined channels for both batch and continuous settling.

Davis and Acrivos (1985) further extend this theory to operation at low Reynolds numbers, while Leung and Probstein (1983) and Probstein et al. (1981) emphasize the design of more efficient settlers.

However, lamella settlers cannot be used to remove particles from colloidal suspensions. Such suspensions are formed in nonaqueous liquids containing asphaltenes. These asphaltenes adsorb on the fine particles present in various liquids of interest in the production of synthetic fuels from coal, oil shale and tar sands, as well as in some oil refining operations. Since the asphaltenes carry a surface charge, a nearly stable colloidal suspension is formed in the presence of a sufficiently high concentration of asphaltenes. Although several approaches can be used to separate these particles, we had previously shown (Lee et al., 1979; Lo et al., 1983) that an effective means to remove such particles is to apply a high-voltage electric field. Previously we had used a cross-flow electrofilter. However, such a device is too expensive to be used in the production of reasonably priced fuels and does not produce a sufficiently concentrated slurry.

A lamella settler, two of whose walls are turned into electrodes, is a much less expensive device and can produce a clarified liquid and a concentrated slurry when operated continuously. In this paper we describe the operation and the hydrodynamic theory of a batch lamella settler with an applied electric field which we call a "lamella electrosettler." This device was tested with a tetralin slurry containing fine alumina particles stabilized with a commercial surfactant, Aerosol OT. Such a system is a model for removal of particles from coal liquids or tar sand extracts, where the surfactant Aerosol OT replaces asphaltenes. This similarity was recently shown in sedimentation tests in cylindrical columns with and without an applied electric field in liquids containing high concentrations of asphaltenes (Shih et al., 1986; Shih, 1986).

The migration of charged particles through aqueous liquids under the influence of an electric field is well known. Shirato et al. (1979) studied the settling rates and consolidation mechanisms of thickened Gairome clay slurries under the influence of a direct electric field. Yukawa et al. (1979) studied an electroosmotic dehydration process of aqueous calcium carbonate and clay suspensions. Stotz (1977), Kuo and Osterle (1967), and Kitahara et al. (1971) also investigated the movement and charge density of particles in very dilute suspensions.

Work on the electrophoretic sedimentation of concentrated nonaqueous systems is quite limited. Lee, Gidaspow and Wasan (1979) conducted test-tube-type electrophoretic sedimentation experiments to separate particles from α-alumina-xylene suspensions. Matsumoto et al. (1981, 1982) experimentally and theoretically studied the electrophoretic sedimentation of fine positively charged oxidized aluminum and iron particles from waste kerosene. Recently, Shih et al. (1987) conducted X-ray-

equipped sedimentation column electrosettling experiments of fine illite particles in toluene with various asphaltene concentrations. This suspension was a model system for some commercial tar sand extracts. They showed that electrosettling was a feasible process for separating fine particles in such nonaqueous media.

Lamella Electrosettling Experiments

Our lamella electrosettler is shown in Figure 1. It is made of 7-mm-thick plexiglas and is in a shape of a rectangular parallepiped. The settler is 60 cm long, has a width of 6 cm and a depth of 8.5 cm. Two 1-mm-thick aluminum electrodes are connected to a high-voltage power supply unit which can generate up to 25 kV of DC voltage and indicate the corresponding current. The electrosettler was mounted on a fixed steel frame at desired inclined angles.

Electrosettling experiments were conducted with α-alumina-tetralin-aerosol OT (dioctyl sodium sulfosuccinate) suspensions. The alumina particles were obtained from a vendor, Agsco Corporation, with a size distribution from 1 to 22 μm. Sufficient aerosol OT was added to the suspension to stabilize the system. Based on the streaming potential measurements and Romm's (1979) interpretation, Chowdiah et al. (1983) estimated the zeta potential for this particular system to be +27.6 mV at 20 mmol/dm^3 aerosol OT concentration. The particles are positively charged. An average particle size of 15 μm and a zeta potential of +30 mV were used for modeling, which are representative values for experiments done over a period of several months. The precise particle size is unimportant, since the electrophoretic mobility is not a strong function of particle size (Mukherjee, 1987). Figure 2 shows typical data reported in Mukherjee's PhD thesis on a liquid similar to tetralin.

Other related electrokinetic parameters, such as the double layer thickness, dielectric constant, and the electrical conductivity of tetralin, were also given by Chowdiah et al. (1981). They are summarized in Table 1 along with the system properties. The initial particle concentration was 1% wt.

The suspension is perfectly stable and settling occurs only when the electric field is applied, whereupon a top sharp interface between the suspension and the particle-free liquid forms almost immediately. A clear visible boundary develops almost instantaneously relative to the settling time beneath the downwards facing electrode, and reaches a steady-state thickness very quickly. Typical photographs of the settling process are shown in Figure 3. The height of the interface was visually obtained as a function of time. The observed behavior was very similar to that of settling of larger particles in a lamella settler under the influence of gravity only, as described by Acrivos and Herbholzheimer (1979). In the case of colloidal particles, however, the driving force is the electric field which is perpendicular to the inclined electrodes. The electric force causes the formation of the thin boundary layer along the face of the top inclined electrode. Gravity and circulation are responsible for the presence of the horizontal interface.

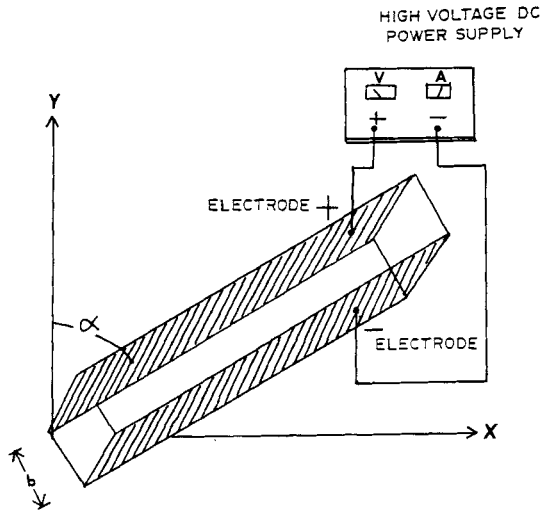

Figure 1. Lamella electrosettler.

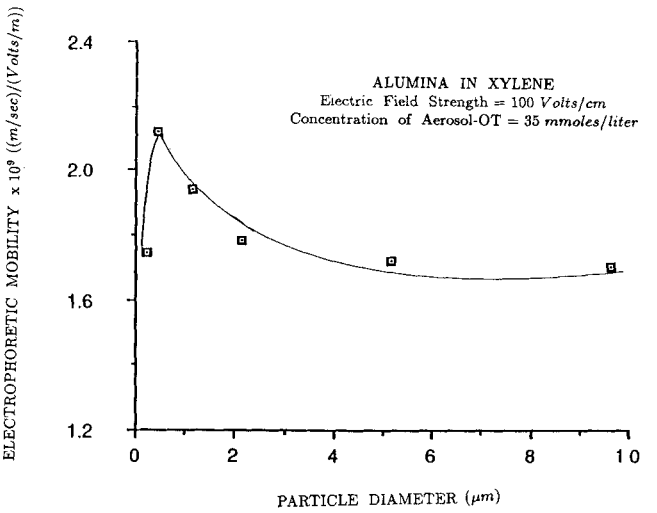

Figure 2. Electrophoretic mobility of particles in xylene.

Experiments were done at various applied electric fields, 250 V/cm to 1,000 V/cm, and at various inclined angles, 40 to 70 degrees (Bouillard, 1986). Typical results are shown in Figure 4, where the dimensionless height, H/H_o is plotted against time. At angles below 40°, no clear interface was observed. In general a higher electric field strength increases the sedimentation rate. For example, at an electric field of 250 V/cm and 50° angle, the settling time was about one hour, whereas at 1,000 V/cm and 70° angle the settling time required only 6 minutes. The settling velocity is shown in Figure 5. For all cases the recorded electrical current requirements were in the range of milliamperes. The power consumption is very small.

Table 1. Electrokinetic Parameters and System Properties of Alumina-Tetralin-Aerosol OT Suspension

Zeta Potential	$\zeta = +30$ mV
Density of Tetralin	$\rho_f = 0.98$ g/cm^3
Viscosity of Tetralin	$\mu_f = 2$ cp
Dielectric Constant of Tetralin	$\bar{\epsilon} = 2.7$
Electrical Conductivity	$K = 1.35 * 10^{-8} \frac{1}{\text{ohmm}}$
Mean Diameter of Particles	$d_p = 15$ μm
Density of Particles	$\rho_s = 3.9$ g/cm^3
Double Layer Thickness	$1/\kappa = 1.2$ μm

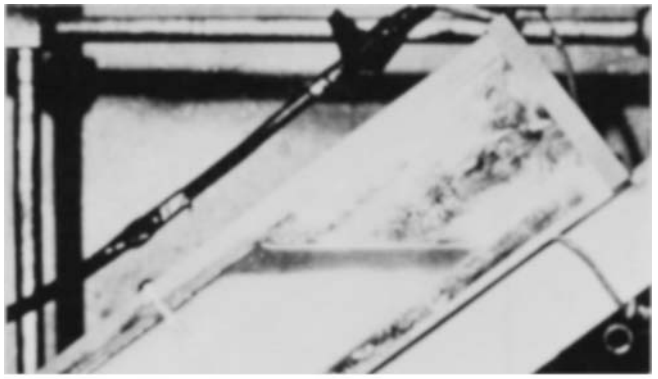

a

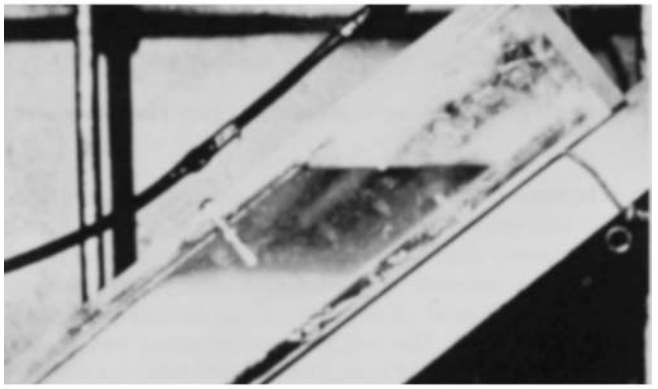

b

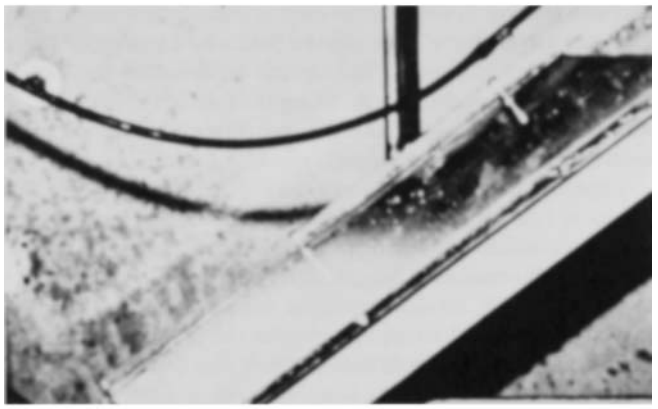

c

Figure 3. Alpha alumina particles (1 μm) settling in a lamella electrosettler after 1 mn (a), 4 mn (b), and 13 mn (c) under 750 V/cm at an inclination angle $\alpha = 50°$.

Approximate settling formula

Acrivos and Herbolzheimer (1979) have discussed the kinematics of commercial-type lamella settlers which they call the PNK theory, crediting Ponder, Nakamura and Kuroda (PNK) for first deriving at an approximate settling formula. We apply such a method to settling enhanced by the electric field. Following Ponder's idea (1925), we express the height of the interface $H(t)$ in terms of the electrophoretic velocity $U_e = Em \cdot E$, where Em is the electrophoretic mobility and E is the strength of the electric field equal to the voltage divided by the distance, and in

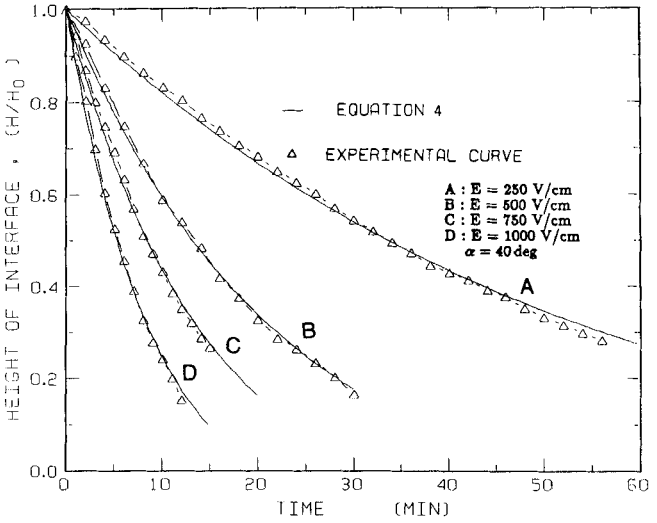

Figure 4. Height of interface vs. time for the system of Table 1 at an inclination angle $\alpha = 40°$; initial height = 39.4 cm.

terms of the gravitational velocity U_o. If we assume the motion of the interface is governed by the motion of the particles at the interface, the volume of clarified liquid produced per unit of time is

$$d/dt \int_{V(t)} dV = \int_{S(t)} \vec{u}_s \cdot \vec{n} dS \tag{1}$$

where u_s is the slip velocity and is given by either U_o or $E_m \cdot E$. In terms of the variables defined in Figure 6, the volume balance given by Eq. 1 can be written as shown below.

$$-\frac{b}{\cos(\alpha)} \frac{dH(t)}{dt} + \int_{S(t)} \vec{u}_s \cdot \vec{n} dS = 0 \tag{2}$$

Noting that u_s is identically zero at the walls, Eq. 2 integrated over the top flat and thin electroboundary layer interfaces gives:

$$\frac{d\bar{H}}{dt} = -(U_o + \sin(\alpha) E_m E) \cdot \left(\frac{1}{H_o} + \frac{U_o \sin(\alpha) + E_m E}{U_o + \sin(\alpha) E_m E} \left(\frac{\bar{H}}{b} \right) \right) \tag{3}$$

where

$$\bar{H} = \frac{H}{H_o} \qquad H_o = H \quad \text{at } t = 0$$

Observing the EE_m/U_o is of the order of 100, if α is not too small, Eq. 3 reduces to a practical electrophoretic settling formula given below.

$$\bar{H}(t) = -\frac{b}{H_o} \sin(\alpha) + \left(1 + \frac{b}{H_o} \sin(\alpha) \right) \exp\left(-\frac{E_m E t}{b} \right) \tag{4}$$

The exponential dependence of H on t is experimentally observed. See Figure 4. From experimental data, the unknown

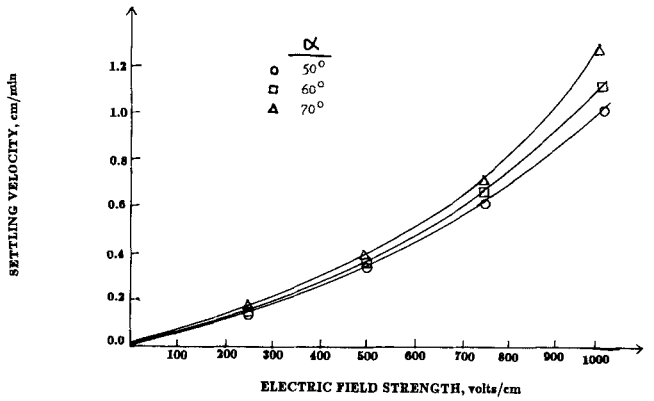

Figure 5. Effect of the electric field strength on the initial settling velocity in a lamella electrosettler.

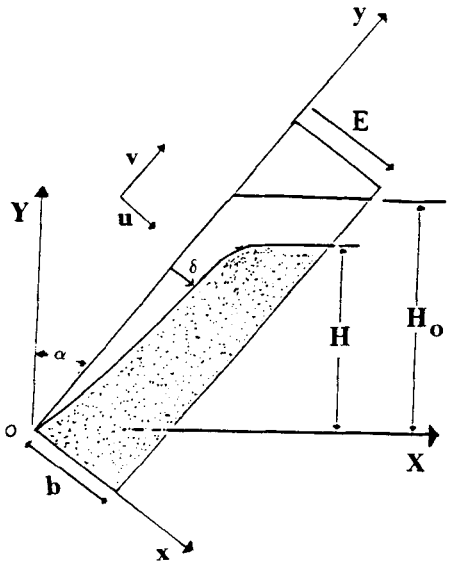

Figure 6. Definition of the variables.

E_m was evaluated for different electric fields by a least square technique, and Eq. 4 was plotted in Figure 4. Figure 7 shows that our electrophoretic mobility compares well with that measured by Lee et al. (1979) at low electric fields using a Zeta meter. Figure 7 shows that the electrophoretic mobility is an increasing function of the electric field strength E. Stotz (1977) found that for a system of polystyrene particles dispersed in water with a chromium anthranilate type of additive his electrophoretic mobility increased with the electric field strength as shown in Figure 7. He further explained that particles, at a high electric field, separate from their double layer and therefore exhibit a higher electrophoretic mobility Em at higher electric field strengths. Hence, the electrophoretic mobility obtained from curve fitting the experimental data gives reasonable values. Furthermore, the kinematic description of the lamella electrosettler can be given by the simple settling formula analogous to the PNK theory.

A Hydrodynamic Model for Lamella Settling and Electrosettling

Hydrodynamic models of sedimentation use the principles of conservation of mass and momentum for each phase. Kos

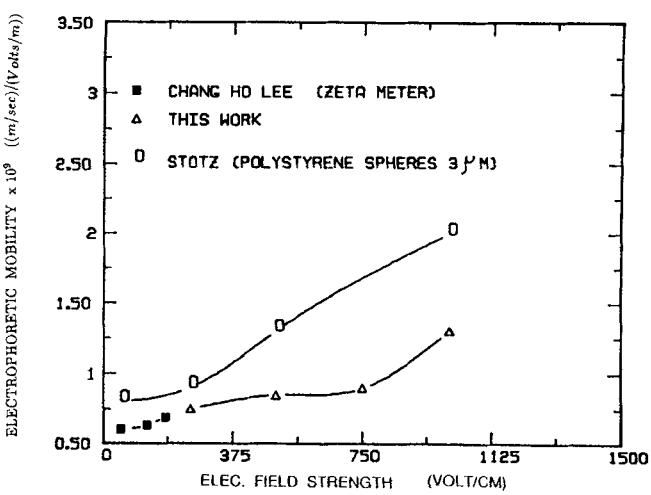

Figure 7. Electrophoretic mobility vs. electric field strength for the system of Table 1.

(1978), Dixon (1980), and Tiller (1981) used general multiphase flow theory to formulate their equations for batch settling. Gidaspow (1986) has recently reviewed such models as they apply to fluidization.

The model developed here for lamella settling or lamella electrosettling is essentially an extension of the K-FIX algorithm (Rivard and Torrey, 1977) developed for gas-liquid flow. The K-FIX computer code was written in a modular form and has been demonstrated to be adaptable to a variety of multiphase problems (Ettehadieh, 1982; Syamlal, 1985). Syamlal (1985) has developed a manual for its use. The K-FIX algorithm was modified to simulate incompressible systems with an externally applied electric force (Shih, 1986).

Governing equations

The lamella settling system considered in this study consists of one incompressible fluid and one particulate phase. Solid particles are assumed to be uniform in size, density, and surface charge. The model can be extended to include N particular phases and granular stresses which have been neglected. The set of governing equations for the lamella settler or the electrosettler is given below.

Continuity Equations

Solid:

$$\frac{\partial}{\partial t}(\rho_s\epsilon_s) + \nabla \cdot (\epsilon_s\rho_s v_s) = 0 \tag{5}$$

Fluid:

$$\frac{\partial}{\partial t}(\rho_f\epsilon_f) + \nabla \cdot (\epsilon_f\rho_f v_f) = 0 \tag{6}$$

Momentum Equations

Solid:

$$\frac{\partial}{\partial t}(\rho_s\epsilon_s v_s) + \nabla \cdot (\epsilon_s\rho_s v_s v_s) = -\epsilon_s\nabla P + \rho_s\epsilon_s g + G_s\nabla\epsilon_f + B_{sf}(v_f - v_s) + \nabla \cdot \epsilon_s\mu_s\nabla v_s + q_v E \tag{7}$$

Fluid:

$$\frac{\partial}{\partial t}(\rho_f \epsilon_f v_f) + \nabla \cdot (\epsilon_f \rho_f v_f v_f) = -\epsilon_f \nabla P + \rho_f \epsilon_f g + B_{fs}(v_s - v_f) + \nabla \cdot \epsilon_f \mu_f \nabla v_f \quad (8)$$

where

ϵ = volume fraction
ρ = density
v = velocity vector
P = pressure
q_v = surface charge of the particles per unit volume
E = strength of the electric field obtained from Maxwell's field equations with an electroneutrality approximation
G_s = elastic modulus for solid phase arising from a force that resists compression
B_{sf}, B_{fs} = drag coefficient to represent the force exerted by the fluid on the particulate solids

The inclined settler is considered to be a two-dimensional system where both the gravitational force g and electrical force E are vector quantities.

Drag law: fluid-particle interaction

There are many correlations in the literature for sedimentation or fluidization velocities of solid-fluid suspensions. For uniform-sized particles, equations suggested by Garside and Al-Dibouni (1977), Barnea and Mizrahi (1973), Wen and Yu (1966), and Richardson and Zaki (1954) were most commonly referenced. In Gidaspow's (1986) review of hydrodynamic modeling of multiphase systems, a fluid-particle correlation was derived from the Ergun equation and Wen and Yu's (1966) formula. This drag relation has been applied in many single- and multiparticulate flowing systems (Gidaspow, 1986). This local drag coefficient was adopted also in the modeling of lamella settlers as follows:

$$B_{fs} = B_{sf} = \frac{150(1-\epsilon_f)\epsilon_s \mu_f}{\epsilon_f (d_p \phi_s)^2} + \frac{1.75 \rho_f |v_f - v_s| \epsilon_s}{(d_p \phi_s)} \quad 0.2 \le \epsilon_f \le 0.8$$

$$= \frac{3}{4} C_{Ds} \frac{\epsilon_f |v_f - v_s| \rho_f \epsilon_s}{(d_p \phi_s)} f(\epsilon_f) \quad 0.8 \le \epsilon_f \le 1.0 \quad (9)$$

where

$$f(\epsilon_f) = \epsilon_f^{-2.65}, \quad (10)$$

$$C_{Ds} = \frac{24}{Re_s}(1 + 0.15 Re_s^{0.687}) \quad Re_s < 1{,}000$$

$$= 0.44, \quad Re_s \ge 1{,}000 \quad (11)$$

and

$$Re_s = \frac{d_p |v_f - v_s| \rho_f \epsilon_f}{\mu_f} \quad (12)$$

Solid compressive stress

In a general formulation, the solid momentum equations would contain solids stress terms that are a function of porosity, pressure and the displacement tensors of solids velocities, gas velocity, and relative velocities. Such a general formulation with proper values of material constants does not exist today (Gidaspow, 1986). From the granular flow theory, only the normal component of the solids stress is retained in this study to prevent the particles from reaching impossibly low values of the void fraction and to provide forces for compression in the sludges. As discussed by Gidaspow and Ettehadieh (1983), such a term is also necessary to make the characteristics real and thereby to make the problem well posed as an initial value problem. Kos (1978) and Shirato et al. (1970) also obtained an empirical relation for the solid stress as a function of solids concentration to use in their models of gravity thickening of sludges.

The solid compressive stress term considered in this model is written in the following form with a stress modulus, $G_s(\epsilon_f)$.

$$G_s(\epsilon_f) \nabla \epsilon_f \quad (13)$$

where $G_s(\epsilon_f)$ is the modulus of elasticity. This equation guarantees the correct direction of solid flows, i.e., in the direction of decreasing solids volume fraction. Shih (1986) obtained this stress modulus by measuring the solid concentration profiles in a sedimentation column at a steady state for a system similar to the one used here. This was done by observing that when there is no motion the solids stress is balanced by buoyancy in the sludge region. (Gidaspow, 1986). The following expression was used for numerical computations.

$$G_s(\epsilon) = -10^{-10.5\epsilon + 9.0} \quad \text{N/m}^2 \quad (14)$$

For the settling of dilute suspensions, this formula gives negligible solid stresses near the clear interface.

Surface charge of particles

To model the lamella electrosettler, we need to know the surface charges of particles. The electric force acting on a particle in an electrostatic field is the product of its charge and the strength of the electric field applied, i.e., $q_v E$ where q_v is the particle surface charge per unit volume of mixture, and E is the externally applied DC field strength (V/cm) which is an experimentally measured value.

Approximate analytical expressions of surface charge density and double-layer potential distributions for a spherical fine particle can be derived by solving the Poisson-Boltzmann equation (Overbeek, 1950; Loeb et al., 1961; Stiger, 1972; Bentz, 1981; Oshima et al., 1982). The Overbeek's (1950) model was adopted in this study due to its simplicity.

His formula for the surface charge of a particle is

$$q_p = 4\pi a_p \bar{\epsilon} \epsilon_o \zeta (1 + \kappa a_p). \quad (15)$$

Therefore,

$$q_v = \left(\frac{\text{No. of Particles}}{\text{Unit Volume}}\right) \quad q_p = \frac{3\bar{\epsilon}\epsilon_o \zeta (1 + \kappa a_p)}{a_p^2} \epsilon_s. \quad (16)$$

For the Alumina-Tetralin-Aerosol OT suspension, the electrokinetic parameters used to describe the surface charge of the particles are listed in Table 1 of the experimental section.

Initial and boundary conditions

A natural initial condition for the lamella settler is that of fully dispersed state. In such a state, the concentration is uniform, and the solid and fluid velocities are zero. For a colloidal suspension, this is exactly true until the electrid field is turned on. The boundary conditions are as given below.

$$\text{B.C. 1:} \quad \text{at } y = 0; \quad V_s = V_f = 0 \tag{17a}$$

$$\text{B.C. 2:} \quad \text{at } y = L_i; \quad P = \text{atmospheric.} \tag{17b}$$

$$\text{B.C. 3:} \quad \text{at } x = 0; \quad U_s = U_f = 0. \tag{17c}$$

$$\text{B.C. 4:} \quad \text{at } x = b; \quad U_s = U_f = 0. \tag{17d}$$

where L_i represents the height of the interface between the suspension and air, and b is the width of the lamella settler. The boundary conditions indicate that no solids or fluid flow through the settler boundaries and that the settler is open to the atmosphere.

Numerical scheme

Governing Eqs. 5 through 8 along with the constitutive equations shown above are solved for v_s, v_f, ϵ_s, ϵ_f, and P using the ICE method (Shih, 1986) The computations were carried out using a mesh of finite difference cells fixed in a two-dimensional space (Eulerian Mesh). The scalar variables are located at the cell center and the vector variables at the cell boundaries.

The continuity equation is differenced fully implicitly, and the flux terms in continuity and momentum equations are full donor-cell-differenced. The donor cell differencing helps to prevent a cell from getting drained completely giving negative volume fractions and also aids in computational stability. The momentum equations are differenced over a staggered mesh of computational cells.

Several modifications were made in this study to the numerical algorithm to simulate the lamella settler with or without an applied electric field. The fluid phase was modified as incompressible, the extra electrical force was included, and the gravitational force was also modified to include the effect of inclined angle of the lamella settler. The pressure and the drag terms remained implicitly differenced; however, the solids stress term was modified to be finite-differenced explicitly to save computational time. Implicitly finite differencing the solids stress term results in more inner loop iterations to meet the convergence criterion. The finite difference equations are solved by a combination of point relaxation, Newton's and Secant iteration method for each computational cell, then by a sweep over the entire settler.

Numerical simulations

Computations for lamella settlers using the numerical algorithm presented in the previous section were carried out for two different systems: for the usual lamella settler which uses gravity as driving force and for the lamella electrosettler which also uses the electrical force. Solid and fluid viscous dissipation terms, $\nabla \cdot \epsilon_s \mu_s \nabla v_s$ and $\nabla \cdot \epsilon_f \mu_f \nabla v_f$, were assumed negligible in all the computations reported here, except for case 2 in Figure 8.

Preliminary measurements with a Weissenberg rheogoniometer indicate that the linear model involving the viscosity of the solid is not an unreasonable approximation of how a solids stress

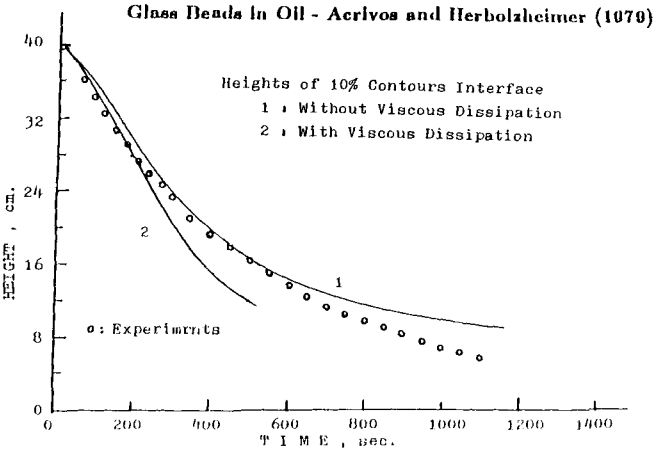

Figure 8. Comparison of computed heights of interfaces in lamella settler.

changes with the gradient of the solids velocity in the shear rate range of 1.5 to 200 s^{-1}, despite the fact that a purely granular flow model for the solids viscosity calls for a square dependence on velocity gradient (Savage and Jeffrey, 1981). The measured viscosity for the mixture was of the order of 25% higher than the viscosity of tetralin. In view of the incompleteness of information obtained so far, effects associated with the sliding of the sludge along the electrodes are not considered here.

Lamella Settler Simulation

One of the typical enhanced settling experiments with lamella settlers is Acrivos and Herbolzheimer's (1979) study. Their settler has a parallel-plate geometry. The length of the plate was 75 cm, and the spacing between the plates was 5 cm. The suspending medium consisted of a mixture of Union Carbide UCON oils and Monsanto HB40 hydrogenated terphenyl oil which gave a Newtonian fluid with density of 0.992 g/mL and a viscosity of 0.677 poises at the nominal temperature of the experiments. The particles were close-sized spherical glass beads with a mean diameter 137 μm and a density of 2.42 g/mL.

The particular experimental condition chosen for numerical simulation of this study is for an initial height, of 40 cm, initial solids concentration of 0.10, and for the inclined angle of 50 degrees. The lamella settler was finite differenced into 393 computational cells. Each cell is 0.833 cm by 1 cm. Simulations were carried out for 1,500 seconds with a time increment of 0.05 seconds. Computations were conducted on supercomputer, CRAY-1. Typical results of simulation are presented below. Shih (1986) gives more detailed comparisons of simulations and experiments.

Concentrations and velocities

The computed solid volume fractions were converted into a series of density plots. The number of black dots is proportional to the volume fraction of solids. Figure 9 shows the concentrations of glass beads at various settling times. Initially, the particles are uniformly dispersed in the settler. At 100 seconds of settling time, the particles are distributed in several regions. Near the top of the suspension, a region of particle-free fluid has formed. A thin particle-free fluid layer beneath the downward-

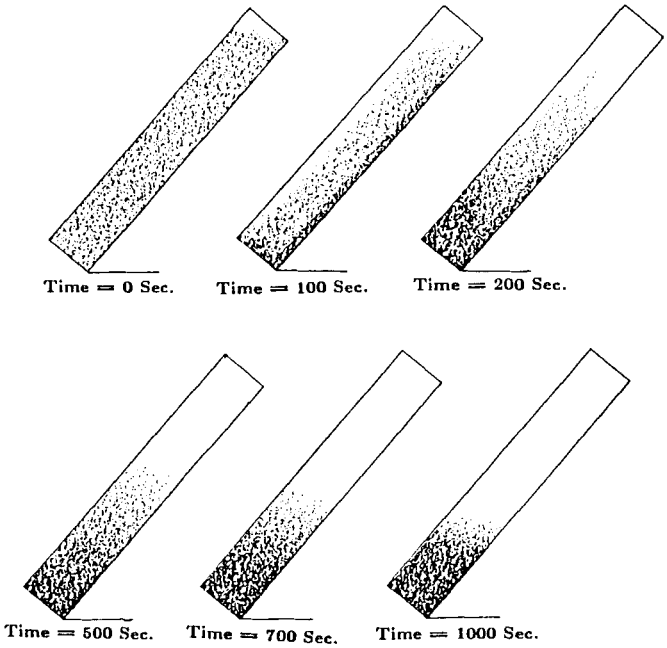

Figure 9. Concentrations of glass beads in a lamella settler at various settling times.

facing surface can also be seen. The concentrated sediment moves toward the bottom and has also formed in a thin layer above the upward-facing plate. Figure 10 shows the motion of the particles at two times. The arrows at the top of the lamella settler show the velocities of the tracer particles left above the interface. Fluid velocities have a similar pattern.

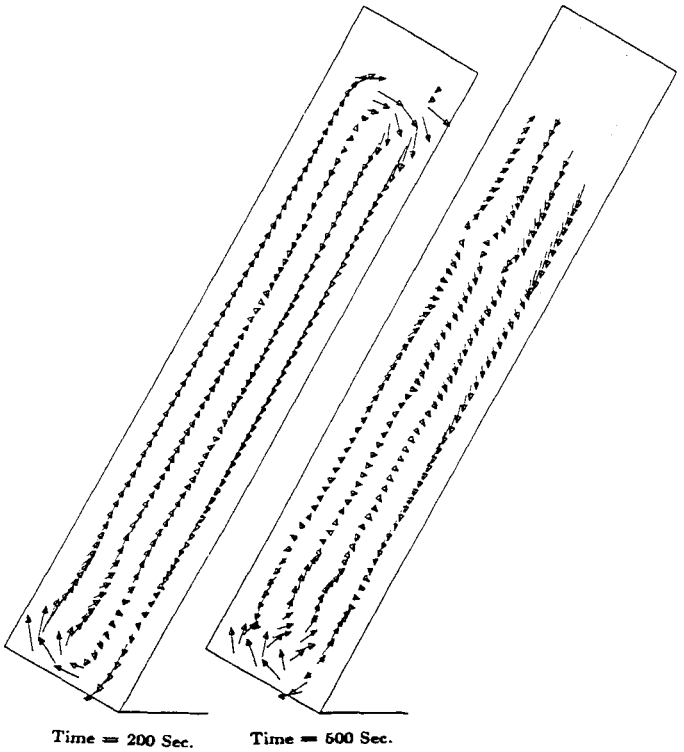

Figure 10. Solid velocity profiles in a lamella settler at various settling times.

Heights of interfaces

Figure 8 shows a comparison of computations to the data of Acrivos and Herbolzheimer (1979). The height of the interface in the simulations was taken to be the initial particle concentration given by the 10% contours. Although all the results reported here are for the inviscid settling, Figure 8 shows the effect of including reasonable estimates of viscosity in the simulations. Although velocities at the wall surfaces are modified by viscosities of the liquid and granular solids sliding down the inclined wall, Figure 8 demonstrates that the rate of settling is not markedly affected.

Electrosettler simulation

Numerical computations for lamella electrosettling were made for two different experiments presented in the previous section for colloidal alumina particles stabilized with Aerosol OT settling in tetralin. The conditions used for the first computer run are as follows: initial height, H_o, = 19.1 cm; initial solids concentration, $\epsilon_{s,o}$ = 0.0025, equivalent to 1 wt. % of solids; inclined angle, α, = 60 degrees; and electric field strength = 750 V/cm. The second run was made with an initial height of 26.8 cm, with an inclined angle of 50 degrees with an electric field strength of 500 V/cm, and with the same initial solid concentration as the first case.

The lamella electrosettler was finite-differenced into 335 computational cells as shown in Figure 11. Each cell is 0.6 cm by 1 cm. Simulations were carried out for 5 minutes with a time increment of 0.001 second. Computations were conducted on supercomputers, CRAY-1 and CRAY 2.

Concentrations and velocities

The computed solid volume fractions were again converted into series of density and contour plots. Figure 12 shows the concentrations of alumina particles at various settling times for an angle of 50° and an electric field of 500 V/cm. Figure 13 shows the solid concentration contours at angle of 60° and for an electric field of 750 V/cm at various settling times. Initially, the particles are uniformly dispersed in the settler. During the pro-

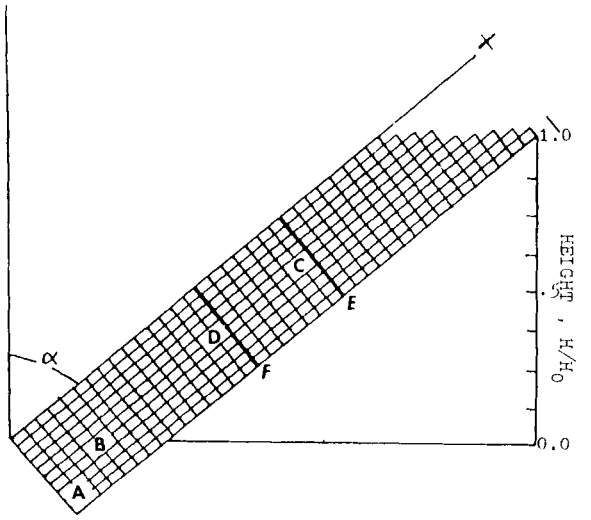

Figure 11. Computational cells in a lamella electrosettler.

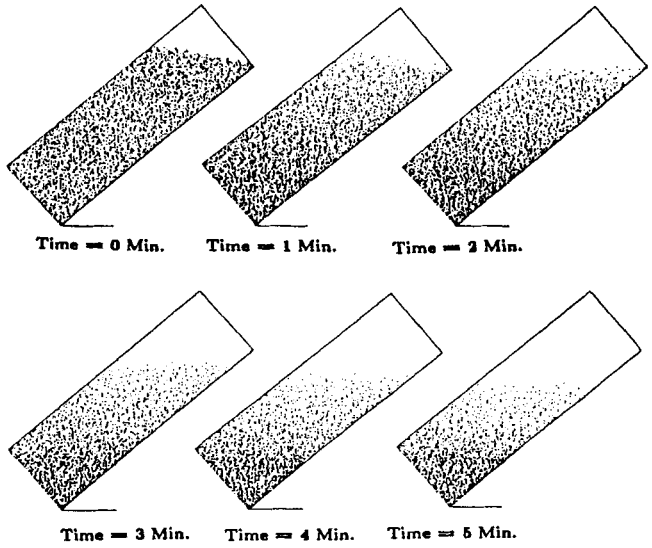

Figure 12. Solid volume fractions in a lamella electrosettler at various times: $\alpha = 50°$ and $E = 500$ V/cm.

cess of electrosettling, several regions can be seen in the settler. They are a particle-free fluid region near the top of settler, a thin particle-free fluid layer beneath the downward-facing surface, concentrated sediments near the bottom and suspensions with varying solids concentrations. The contour plots clearly show the thin boundary layer and indicate that there is a variation of solid concentrations in the suspension and sediments. Although there were no experimentally measured concentration profiles to verify the variations, our pictures of electrosettling did show the diluteness near the top of the suspension. In the sediment layer, we used our X-ray technique to measure concentration profiles (Shih, 1986). Convective solids circulations in the settler and crude discretization in numerical computations required by necessity of reasonable computer time may both contribute to this phenomenon.

Solid and fluid flow patterns for the lamella electrosettler

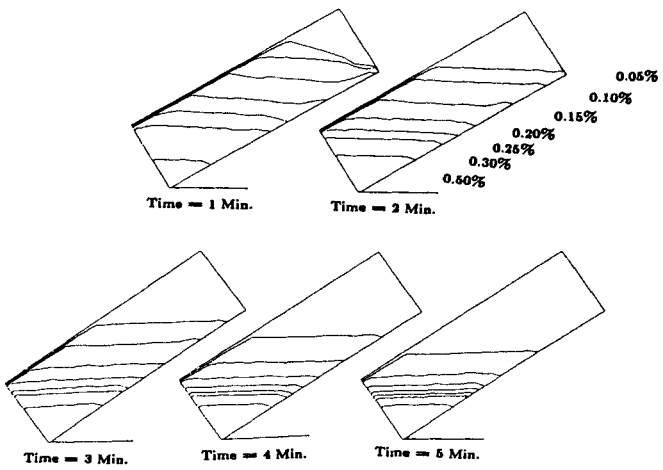

Figure 13. Solid concentration contours in a lamella electrosettler at various times: $\alpha = 60°$, $E = 750$ V/cm.

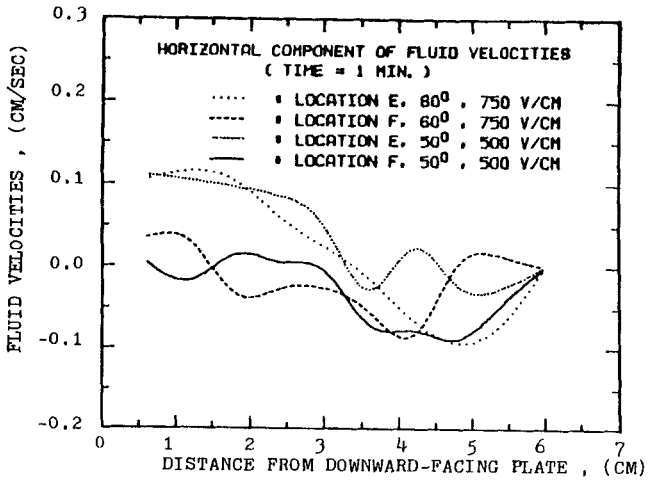

Figure 14. Horizontal component of solid velocities across a lamella electrosettler at different operating conditions.

were similar to those already shown for the lamella settler. There was a somewhat greater circulation in the core of the electrosettler (Shih, 1986). Typical components of the solid velocities at the locations indicated in Figure 11 are shown in Figures 14 and 15. Both the fluid and the solid velocities are upward near the positive electrode and downward near the negative electrode, caused by the sliding of the solids along the bottom electrode. The velocities in the center of the cell are small compared with those at the faces of the electrodes.

Heights of interfaces

From the solid concentration profiles, the heights of "particle-free" interfaces were plotted in Figures 16 and 17 to compare with the experimental observations. The computed interfaces were represented by 0.08% contours. Reasonable agreement was obtained for both runs. At the initial stage of settling, the model

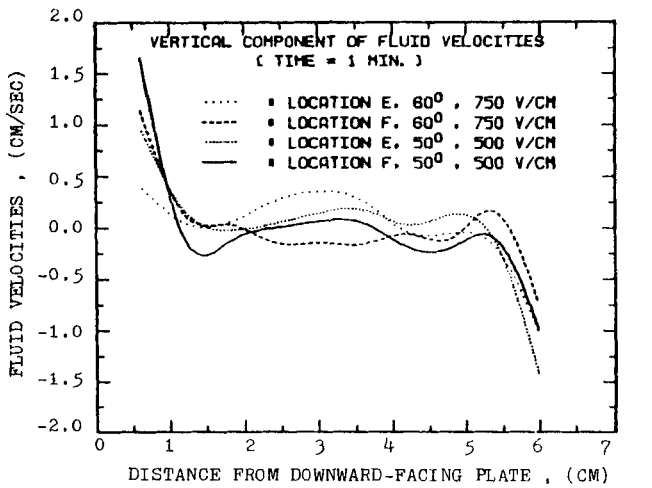

Figure 15. Vertical component of solid velocities across a lamella electrosettler at different operating conditions.

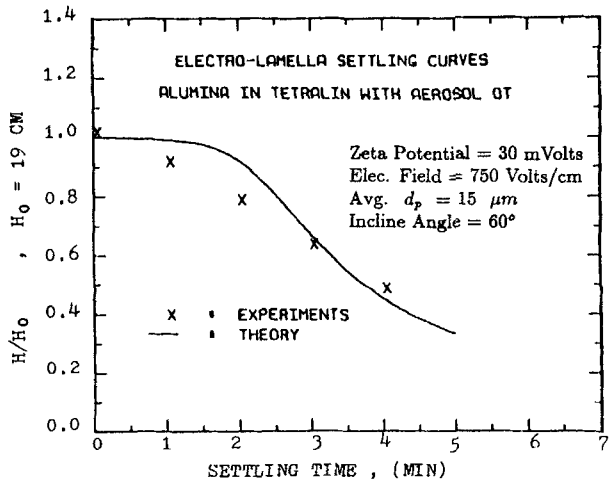

Figure 16. Settling curves of an alumina-tetralin-AOT system: theory vs. experiment, α = 60° and E = 750 V/cm.

predicted slower settling rates and at the later stage, the computed settling rate was slightly higher.

Boundary layer thickness

The thickness of the clear fluid layer beneath the downward-facing plate observed in experiments, for 50° inclination and 500 V/cm, was compared with the 0.05% and 0.1% contours computed by the model for lamella electrosettling. Figure 3 was enlarged to measure the particle-free boundary layer thickness. At half of the vertical height, the measured thickness was about 0.11 cm. There were no significant variations at various settling times. The computed distances from the surface of the downward-facing plate to the interfaces of the 0.05% and 0.1% contours at half-height of the suspension were 0.12 cm and 0.19 cm, respectively. Similar to the analysis for lamella settling, these distances were obtained by interpolation to the nearest computational cell. The boundary layer thickness observed in experiments was approximately the calculated distance between the downward-facing plate and the 0.5% contour.

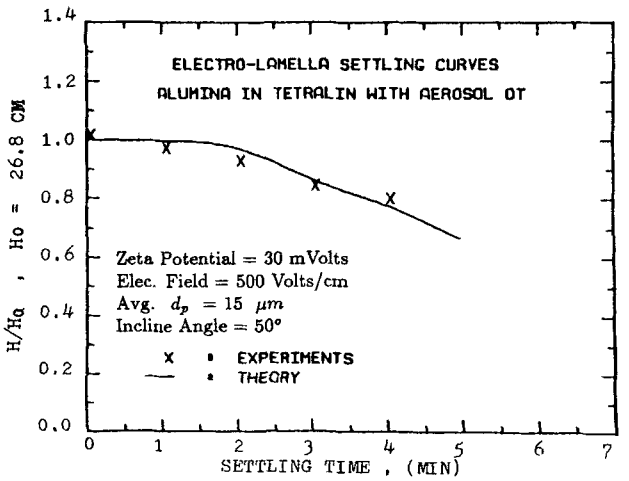

Figure 17. Settling curves of an alumina-tetralin-AOT system: theory vs. experiment, α = 50° and E = 500 V/cm.

Asymptotic Electroboundary Layer

The stretched variable asymptotic technique of Acrivos and Herbolzheimer (1979) was applied to the case of electrosettling for obtaining the particle free layer below the top electrode. The same assumptions were made. The major difference is in the boundary condition two, BC-2 in Table 2. This boundary condition replaces the boundary condition given by Eqs. 3 and 4b of Acrivos and Herbolzheimer (1979). Bouillard (1986) shows

Table 2. Hydrodynamic Model for Boundary Layer Analysis

Continuity Equation

$$\frac{\partial \tilde{u}}{\partial \tilde{x}} + \frac{\partial \tilde{v}}{\partial \tilde{y}} = 0$$

Momentum Equation

$$R\frac{d\bar{u}}{d\bar{t}} = -\bar{\nabla}\bar{P} - \Lambda\left(\frac{\rho_f}{c_o(\rho_s - \rho_f)}\right)\bar{g} + \bar{\mu}\,\bar{\nabla}^2\bar{u}$$

Reduced Momentum Equations

$$\frac{\partial^2 \tilde{v}}{\partial \tilde{x}^2} + \cos\alpha - \frac{1}{\Lambda}\frac{\partial \bar{P}}{\partial \tilde{y}} = R\Lambda^{-1/3}\left(\tilde{u}\frac{\partial \tilde{v}}{\partial \tilde{x}} + \tilde{v}\frac{\partial \tilde{v}}{\partial \tilde{y}}\right) + O(R\Lambda^{-2/3}) + O(\Lambda^{-1/3})$$

$$\Lambda^{-2/3}\frac{\partial \bar{P}}{\partial \tilde{x}} + \sin\alpha = O(\Lambda^{-1/3}) + O(R\Lambda^{-2/3})$$

Boundary Conditions

BC-1 $\quad \tilde{u} = \tilde{v} = 0 \quad$ at $\quad \tilde{x} = 0$

BC-2 $\quad \Lambda^{-1/3}\frac{\partial \tilde{\delta}}{\partial \bar{t}} + \tilde{v}\frac{\partial \tilde{\delta}}{\partial \tilde{y}} - \tilde{u} = \frac{U_o \sin\alpha + E_m E}{v_o} \quad$ at $\quad \tilde{x} = \tilde{\delta}$

BC-3 $\quad \frac{\partial \tilde{v}}{\partial \tilde{x}} = o(1) \quad$ at $\quad \tilde{x} = \tilde{\delta}$

Dimensionless Factors with Similarity Transforms

Dimensionless Factors	Similarity Transforms
$\bar{x} = \frac{x}{H_o}, \quad \bar{y} = \frac{y}{H_o}, \quad \bar{t} = \frac{v_o t}{H_o}$	$\tilde{x} = \Lambda^{1/3}\bar{x}, \quad \tilde{y} = \bar{y}$
$\bar{u} = \frac{u}{v_o}, \quad \bar{v} = \frac{v}{v_o}, \quad \bar{p} = \frac{H_o p}{\mu v_o}$	$\tilde{u} = \bar{u}, \quad \tilde{v} = \Lambda^{-1/3}\bar{v}$
$\bar{g} = \frac{g}{\lvert g\rvert}, \quad R = \frac{\rho_f v_o H_o}{\mu}$	$\tilde{\delta} = \frac{\Lambda^{1/3}\delta}{H_o}$
$G = \frac{H_o^3(\rho_s - \rho_f)g c_o \rho_f}{\mu^2}, \quad \Lambda = \frac{H_o^2(\rho_s - \rho_f)g c_o}{\mu v_o}$	
$v_o = U_o + E_m E, \quad \bar{\mu} = \frac{\mu_s}{\mu}$	
$\bar{\nabla}\bar{P} = \bar{\nabla}\bar{p} - \Lambda\left(1 + \frac{\rho_f}{c_o(\rho_s - \rho_f)}\right)\bar{g}$	

that the electroboundary layer thickness becomes:

$$\tilde{\delta} = \left(\frac{3}{\cos(\alpha)}\left(\frac{U_o \sin(\alpha) + E_m E}{U_o + E_m E}\right)x\right)^{1/3} \tag{18}$$

After dropping the gravitational velocity u_o terms compared with the electrophoretic velocity EmE, δ can be written as follows:

$$\delta = \left(\frac{3E_m E_\mu}{c_o \cos\alpha(\rho_s - \rho_f)g}\right)^{1/3} y^{1/3} \tag{19}$$

We found a good agreement with the predicted electroboundary layer thickness of 1.2 mm at 500 V/cm and the experimental thickness of 1.1 mm. For very high electric field strengths, the assumptions made in the asymptotic solution may not apply any longer (Bouillard, 1986).

Conclusions

- A new and useful device for separating colloidal particles suspended in nonaqueous media was developed and illustrated with a system that is a model for separating particles from coal-liquefaction slurries.
- A kinematic-type settling formula was developed for this device, called the lamella electrosettler, which predicts settling rates in terms of an electrophoretic mobility of the colloidal particles.
- A computer hydrodynamic model was developed for a lamella settler which predicts settling behavior and flow patterns. The input into the model involves only the standard drag law relations for spherical particles and flow in porous media and powder stress moduli in the sludge regions of the settler.
- The hydrodynamic computer model was shown to describe the flow and settling behavior in the lamella electrosettler. The additional input into the model involves the electrophoretic mobility of the particles in the nonaqueous medium or their zeta potentials which much be measured separately.

Acknowledgment

This study was supported by the National Science Foundation through an Industry-University Cooperative Research Program with the Amoco Corporation. Mr. D. Foote performed the electrolamella settling experiments as part of a research project for a nonthesis Master's degree in chemical engineering.

Notation

a_p = solid particle radius
B = local mean drag coefficient
b = space between inclined plates
C_D = drag coefficient
c = initial volume fraction of solids
d_p = solid particle diameter
E = externally applied electric field strength
E_m = electrophoretic mobility
f = function defined by Eq. 10
G_s = solids compressive stress modulus
G = sedimentation Grashof number
g = gravitational acceleration
$H(t)$ = height of the clear interface
H_o = initial interface height
$\overline{H} = (H/H_o)$ = interface height
$\underline{K}$ = liquid electric conductivity, mho/m
$\vec{n}$ = outward drawn normal
P = system Pressure
$\bar{p}$ = pressure
q_p = surface charge of a particle
q_v = surface charge per unit volume of mixture
R = sedimentation Reynolds number
R_e = Reynolds number
S = surface
t = time
U_s = velocity component of solid in the x direction
U_f = velocity component of fluid in the x direction
U_e = electrophoretic velocity
U_o = gravitational velocity
u_s = slip velocity
V = volume
V_f = velocity component of fluid in the y direction
V_s = velocity component of solid in the y direction
v = phase velocity
v_o = settling velocity at zero degree inclined angle
x = lateral coordinate
y = vertical coordinate

Greek letters

α = inclined angle
δ = boundary layer thickness
ϵ = volume fraction
μ = viscosity
ϕ = shape factor of solids
ρ = density
$\Lambda = G/R$ = ratio of sedimentation Gr to sedimentation Re numbers
ζ = zeta potential
$\bar{\epsilon}$ = dielectric constant of the liquid
$\bar{\epsilon}_o$ = permittivity of vacuum
κ = inverse of double layer thickness

Subscripts

f = fluid phase
o = initial status
s = solid phase, unless indicated otherwise

Literature Cited

Acrivos, A., and E. Herbolzheimer, "Enhanced Sedimentation in Settling Tanks with Inclined Walls," *J. Fluid Mech.*, **92,** 435 (1979).

Barnea, E., and J. Mizrahi, "A Generalized Approach to the Fluid Dynamics of Particulate Systems: I. General Correlation for Fluidization and Sedimentation in Solid Multiparticle Systems," *Chem. Eng. J.*, **5,** 171 (1973).

Bentz, J., "Electrostatic Potential Around a Charged Sphere with Cation Binding," *J. Coll. Interf. Sci.*, **80,** 179 (1981).

Bouillard, J., "Hydrodynamics of Sedimentation, Fluidization and Erosion," PhD Thesis, Ill. Inst. of Technol., Chicago (1986).

Chowdiah, P., D. T. Wasan, and D. Gidaspow, "On the Interpretation of Streaming Potential Data in Non-Aqueous Media," *Colloids and Surfaces*, **7,** 291 (1983).

Chowdiah, P., D. T. Wasan, and D. Gidaspow, "Electrokinetic Phenomena in the Filtration of Colloidal Particles Suspended in Non-Aqueous Media," *AIChE J.*, **27,** 975 (1981).

Davis, R. H., and A. Acrivos, "Sedimentation of Noncolloidal Particles at Low Reynolds Number," *Ann. Rev. Fluid Mech.*, **17,** 91 (1985).

Davis, R. H., E. Herbolzheimer, and A. Acrivos, "Wave Formation and Growth During Sedimentation in Narrow Tilted Channels," *Phys. Fluids*, **26,** 2055 (1983).

Dixon, D. C., "Effect of Sludge Funneling in Gravity Thickeners," *AIChE J.*, **26,** 471 (1980).

Ettehadieh, B., "Hydrodynamic Analysis of Gas-Solid Fluidized Beds," PhD Diss., Ill. Inst. of Technol. (1982).

Forsell, B., and B. Hedstrom, "Lamella Sedimentation: A Compact Separation Technique," *J. WPCF*, **47**(4), 834 (1975).

Garside, J., and M. R. Al-Dibouni, "Velocity-Voidage Relationship for Fluidization and Sedimentation in Solid-Liquid Systems," *Ind. Eng. Chem., Process Des. Dev.*, **16,** 206 (1977).

Gidaspow, D., "Hydrodynamics of Fluidization and Heat Transfer: Supercomputer Modeling," *Appl. Mech. Rev.*, **39,** 1 (1986).

Gidaspow, D., and B. Ettehadieh, "Fluidization in Two-Dimensional Beds with a Jet. 2. Hydrodynamic Modeling," *Ind. Eng. Chem. Fund.*, **22**, 193 (1983).
Gidaspow, D., and M. Syamlal, "Solid-Gas Critical Flow," AIChE Meeting, paper no. 74e, Chicago (Nov., 1985).
Herbolzheimer, E., and A. Acrivos, "Enhanced Sedimentation in Narrow Tilted Channels," *J. Fluid Mech.*, **108**, 845 (1981).
Hill, W. D., "Boundary-Enhanced Sedimentation due to Settling Convection," PhD Thesis, Carnegie-Mellon Univ., Pittsburgh (1974).
Hill, W. D., R. R. Rothfus, and K. Li, "Boundary Enhanced Sedimentation Due to Settling Convection," *Int. J. Multiphase Flow*, **3**, 561 (1977).
Kithara, A., T. Fujii, and S. Katano, "Dependence of ζ-Potential upon Particle Size and Capillary Radius at Streaming Potential Study in Nonaqueous Media," *Bull. Chem. Soc. Jpn.*, **44**, 3242 (1971).
Kos, P., "Gravity Thickening of Sludges," PhD Thesis, Univ. of Mass. (1978).
Kuo, S., and F. Osterle, "High Field Electrophoresis in Low Conductivity Liquids," *J. Colloid Interf. Sci.*, **25**, 421 (1967).
Lee, C., D. Gidaspow, and D. T. Wasan, *Proc. Technical Program of Int. Powder and Solids Handling and Process.*, 528, Philadelphia (May, 1979).
Lo, Y. S., D. Gidaspow, and D. T. Wasan, "Separation of Colloidal Particles from Nonaqueous Media by Cross-Flow Filtration," *Separ. Sci.*, **18**, 1323 (1983).
Leung, W. F., and R. F. Probstein, "Lamella and Tube Settlers: I. Model and Operation," *Ind. Eng. Chem. Process Des. Dev.*, **22**, 58 (1983).
Loeb, A. L., J. Th. G. Overbeek, and P. H. Wiersema, "The Electrical Double Layer Around a Spherical Colloidal Particle," MIT Press, Cambridge, MA (1961).
Mukherjee, A., "Characterization and Separation of Charged Particles," PhD Thesis, Ill. Inst. of Technol., Chicago (1987).
Matsumoto, K., O. Kutowy, and C. E. Capes, "An Experimental Investigation of the Electrophoretic Sedimentation of Fine Particles in Waste Kerosene," *Powder Technol.*, **28**, 205 (1981).
Matsumoto, K., O. Kutowy, and C. E. Capes, "Some Theoretical Aspects of the Electrophoretic Sedimentation of Particles," *Powder Technol.*, **31**, 197 (1982).
Nakamura, N., and K. Kuroda, "La Cause de l'Acceleration de la Vitesse de Sedimentation des Suspensions dans les Recipients Inclines," *Keijo J. Med.*, **8**, 256 (1937).
Oshima, H., T. W. Healy, and L. R. White, "Accurate Analytic Expressions for the Surface Charge Density/Surface Potential Relationship and Double Layer Potential Distribution for a Spherical Colloidal Particle," *J. Colloid Interf. Sci.*, **90**, 17 (1982).
Overbeek, J. Th. G., *Adv. Colloid Sci.*, **3**, (1950), cited by G. D. Parfitt and J. Peacock, "Stability of Colloidal Dispersions in Nonaqueous Media," *Surf. and Colloid Sci.*, **10**, 163 (1978).
Ponder, E., "On Sedimentation and Rouleaux Formation," *Q. J. Exp. Physiol.*, **15**, 235 (1925).
Probstein, R. F., R. Yung, and R. Hicks, "A Model for Lamella Settlers," *Phys. Separ.*, eds. Freeman, M. P., and Fitzpatrick, J. A., 33–52, Eng. Found., New York, 1981.
Richardson, J. F., and W. N. Zaki, "Sedimentation and Fluidization: Part I," *Trans. Inst. Chem. Eng.*, **32**, 35 (1954).
Rivard, W. C., and M. D. Torrey, "K-FiX: A Computer Program for Transient Two Dimensional Two Fluid Flow," LA-NUREG-6623, Los Alamos (1977).
Romm, E. S., "Characteristics of Electrokinetic Phenomena in Fine Capillaries," *Colloid J. of U.S.S.R.*, English Translation, **41**, 758 (1979).
Rubinstein, I., "A Steady Lamella Flow of Suspension in a Channel," *Int. J. Multiphase Flow*, **6**, 473 (1980).
Savage, S. B., and D. J. Jeffrey, "The Stress Tensor in Granular Flow at High Shear Rates," *J. Fluid Mech.*, **110**, 255 (1981).
Schaflinger, W., "Experiments on Sedimentation Beneath Downward-Facing Inclined Walls," *Int. J. Multiphase Flow*, **11**(2), 189 (1985).
Schneider, W., 'Kinematic—Wave Theory of Sedimentation Beneath Inclined Walls," *J. Fluid Mech.*, **120**, 323 (1982).
Shih, Y. T., "Hydrodynamics of Separation of Particles: Sedimentation and Fluidization," PhD Thesis, Ill. Inst. of Technol., Chicago (1986).
Shih, Y. T., D. Gidaspow, and D. T. Wasan, "Sedimentation of Fine Particles in Nonaqueous Media," *Colloids and Surfaces*, **21**, 383 (1986).
Shirato, M., T. Aragaki, A. Manabe, and N. Takeuchi, "Electroforced Sedimentation of Thick Clay Suspensions in Consolidation Region," *AIChE J.*, **25**, 855 (1979).
Shirato, M., H. Kato, K. Kobayashi, and H. Sakazaki, "Analysis of Settling of Thick Slurries due to Consolidation," *J. of Chem. Eng. of Japan*, **3**, 98 (1970).
Stiger, D., *J. Electroanal. Chem.*, **37**, 61 (1972), cited by H. Oshima, T. W. Healy, and L. R. White, "Accurate Analytic Expressions for the Surface Charge Density/Surface Potential Relationship and Double Layer Potential Distribution for a Spherical Colloidal Particle," *J. Colloid Interf. Sci.*, **90**, 17 (1982).
Stotz, S., "Field Dependence of the Electrophoretic Mobility of Particles Suspended in Low Conductivity Liquids," *J. Colloid Interf. Sci.*, **65**, 118 (1977).
Syamlal, M., "Multiphase Hydrodynamics of Gas-Solids Flow," PhD Thesis, Ill. Inst. of Technol., Chicago (1985).
Tiller, F. M., "Revision of Kynch Sedimentation Theory," *AIChE J.*, **27**, 823 (1981).
Wen, C. Y., and Y. H. Yu, "Mechanics of Fluidization," *AIChE Symp. Ser.*, No. 62, 100 (1966).
Yukawa, H., K. Kobayashi, H. Yoshida, and M. Iwata, "Progress in Filtration and Separation," 83, Elsevier, New York (1970).
Zahavi, E., and E. Rubin, "Settling of Solid Suspensions Under and Between Inclined Surfaces," *Ind. Eng. Chem. Process Des. Dev.*, **14**(1), 34 (1975).

Manuscript received Mar. 14, 1988, and revision received Aug. 25, 1988.